



HAL
open science

Combined anti-fibrotic and anti-inflammatory properties of JAK-inhibitors on macrophages in vitro and in vivo perspectives for scleroderma-associated interstitial lung disease

Alain Lescoat, Marie Lelong, Mohamed Jeljeli, Claire Piquet-Pellorce, Claudie Morzadec, Alice Ballerie, Stéphane Jouneau, Patrick Jego, Laurent Vernhet, Frédéric Batteux, et al.

► To cite this version:

Alain Lescoat, Marie Lelong, Mohamed Jeljeli, Claire Piquet-Pellorce, Claudie Morzadec, et al.. Combined anti-fibrotic and anti-inflammatory properties of JAK-inhibitors on macrophages in vitro and in vivo perspectives for scleroderma-associated interstitial lung disease. *Biochemical Pharmacology*, 2020, 178, pp.114103. 10.1016/j.bcp.2020.114103 . hal-02888737

HAL Id: hal-02888737

<https://hal.science/hal-02888737v1>

Submitted on 9 Jul 2020

HAL is a multi-disciplinary open access archive for the deposit and dissemination of scientific research documents, whether they are published or not. The documents may come from teaching and research institutions in France or abroad, or from public or private research centers.

L'archive ouverte pluridisciplinaire **HAL**, est destinée au dépôt et à la diffusion de documents scientifiques de niveau recherche, publiés ou non, émanant des établissements d'enseignement et de recherche français ou étrangers, des laboratoires publics ou privés.

BIOCHEMICAL PHARMACOLOGY

Category: Inflammation and Immunopharmacology

Full-length Research Article

Combined anti-fibrotic and anti-inflammatory properties of JAK-inhibitors on macrophages in vitro and in vivo: perspectives for scleroderma-associated interstitial lung disease.

Alain LESCOAT^{1,2}, Marie LELONG¹, Mohamed JELJELI^{3,4}, Claire PIQUET-PELLORCE¹, Claudie MORZADEC¹, Alice BALLERIE^{1,2}, Stéphane JOUNEAU^{1,5}, Patrick JEGO^{1,2}, Laurent VERNHET¹, Frédéric BATTEUX^{3,4}, Olivier FARDEL^{1,6} and Valérie LECUREUR^{1*}

1-Univ Rennes, CHU Rennes, Inserm, EHESP, Irset (Institut de recherche en santé, environnement et travail) – UMR_S 1085, F-35000 Rennes, France

2-Department of Internal Medicine and Clinical Immunology, Rennes University Hospital, 35203, Rennes, France.

3 Institut Cochin, INSERM U1016, Université Paris Descartes, Sorbonne Paris Cité, Paris, France.

4 Assistance Publique–Hôpitaux de Paris (AP–HP), Hôpital Universitaire Paris Centre (HUPC), Centre Hospitalier Universitaire (CHU) Cochin, Service d’immunologie biologique (Professeur Batteux), Paris, France.

5- Department of Respiratory Diseases, Rennes University Hospital, 35203, Rennes, France.

6-Pôle Biologie, Rennes University Hospital, 35203, Rennes, France

***Corresponding author** : Dr Valérie LECUREUR, Institut de Recherche en Santé, Environnement et Travail (IRSET-INSERM UMR 1085), Université de Rennes 1, 2 avenue du Pr Léon Bernard, 35043 Rennes cedex, France. Phone: 33-2-23-23-47-88; Fax: 33-2-23-23-47-94. Email: valerie.lecureur@univ-rennes1.fr

Word count: 5764 words; 9 figures ; 54 references

Category: Inflammation and Immunopharmacology

Conflict of interest: the authors have no conflict of interest to declare.

ABSTRACT

Janus kinase (JAK) inhibitors (also termed Jakinibs) constitute a family of small drugs that target various isoforms of JAKs (JAK1, JAK2, JAK3 and/or tyrosine kinase 2 (Tyk2)). They exert anti-inflammatory properties linked, in part, to the modulation of the activation state of pro-inflammatory M1 macrophages. The exact impact of JAK inhibitors on a wider spectrum of activation states of macrophages is however still to be determined, especially in the context of disorders involving concomitant activation of pro-inflammatory M1 macrophages and profibrotic M2 macrophages. This is especially the case in autoimmune pulmonary fibrosis like scleroderma-associated interstitial lung disease (ILD), in which M1 and M2 macrophages play a key pathogenic role. In this study, we directly compared the anti-inflammatory and anti-fibrotic effects of three JAK inhibitors (ruxolitinib (JAK2/1 inhibitor); tofacitinib (JAK3/2 inhibitor) and itacitinib (JAK1 inhibitor)) on five different activation states of primary human monocyte-derived macrophages (MDM). These three JAK inhibitors exert anti-inflammatory properties towards macrophages, as demonstrated by the down-expression of key polarization markers (CD86, MHCII, TLR4) and the limited secretion of key pro-inflammatory cytokines (CXCL10, IL-6 and TNF α) in M1 macrophages activated by IFN γ and LPS or by IFN γ alone. We also highlighted that these JAK inhibitors can limit M2a activation of macrophages induced by IL-4 and IL-13, as notably demonstrated by the down-regulation of the M2a associated surface marker CD206 and of the secretion of CCL18. Moreover, these JAK inhibitors reduced the expression of markers such as CXCL13, MARCO and SOCS3 in alternatively activated macrophages induced by IL-10 and dexamethasone (M2c+dex) or IL-10 alone (M2c MDM). For all polarization states, Jakinibs with inhibitory properties over JAK2 had the highest effects, at both 1 μ M or 0.1 μ M. Based on these *in vitro* results, we also explored the effects of JAK2/1 inhibition by ruxolitinib *in vivo*, on mouse macrophages in a model of HOC1-induced ILD, that

mimics scleroderma-associated ILD. In this model, we showed that ruxolitinib significantly prevented the upregulation of pro-inflammatory M1 markers (TNF α , CXCL10, NOS2) and pro-fibrotic M2 markers (Arg1 and Chi3L3). These results were associated with an improvement of skin and pulmonary involvement. Overall, our results suggest that the combined anti-inflammatory and anti-fibrotic properties of JAK2/1 inhibitors could be relevant to target lung macrophages in autoimmune and inflammatory pulmonary disorders that have no efficient disease modifying drugs to date.

Keywords: Inflammation, Interstitial Lung disease, Janus kinase inhibitors, macrophage activation, Systemic sclerosis

1. Introduction

Janus kinase (JAK) inhibitors (also termed Jakinibs (1)) constitute a family of small drugs that target various isoforms of JAK (notably JAK1, JAK2, JAK3 and/or tyrosine kinase 2 (Tyk2)) (2). JAK2 inhibitors, such as ruxolitinib, were initially used in the treatment of JAK2 V617F myeloproliferative disorders (3). Due to their anti-inflammatory properties, JAK inhibitors such as tofacitinib (JAK3 and 2 inhibitor) and baricitinib (JAK2 and 1 inhibitor) are now also approved for the treatment of rheumatoid arthritis (4,5). These effects of tofacitinib and baricitinib in rheumatoid arthritis are especially mediated through their impact on the plasma levels of pro-inflammatory cytokines such as IL-6 and IL-17, that play an important role in the immune-mediated inflammatory manifestations of this autoimmune connective tissue disease (6,7). Beyond these anti-inflammatory effects, JAK inhibitors could also exert anti-fibrotic properties (8), possibly due to their direct impact on fibroblast activation (9), in various fibrotic disorders, such as autoimmune liver fibrosis or idiopathic pulmonary fibrosis (8,10,11). Nonetheless, the precise cellular targets of JAK inhibitors are still to be further explored, specifically in the context of fibrotic and autoimmune diseases (12). So far, the evaluation of the effects of JAK inhibitors and JAK/STAT pathways in autoimmune diseases has mainly focused on their anti-inflammatory properties. Some authors consider that Jakinibs could become the main pharmacological therapeutic class for autoimmune diseases, specifically highlighting that they are oral treatments contrarily to biologics (13). Moreover, “a post-biologics era” in Rheumatology and autoimmunity may begin when the patents of synthetic Jakinibs expire (13). Thus, the evaluation of other properties of JAK inhibitors in the field of autoimmune diseases, beyond their anti-inflammatory properties and their effects on autoimmune-related inflammatory manifestations, is particularly significant.

Interestingly, as demonstrated by our team, the anti-inflammatory properties of JAK inhibitors are, in part, the results of their effects on the activation state of pro-inflammatory

macrophages with a down-regulation of interferon β (IFN β) signature and IL-6 expression (14). It is noteworthy that macrophages can adopt various activation profiles, depending on their surrounding microenvironment and cytokinic stimuli, which range from pro-inflammatory (classical M1 macrophages) to anti-inflammatory states (alternative M2 macrophages) with pro-fibrotic properties (15). M1 macrophage activation is classically the result of TLR4 and/or IFN γ signaling, with the direct involvement of JAK1/JAK2/P-STAT1 pathway, through the activation of the IFN γ receptor. IL-10 signaling drives the differentiation of M2 anti-inflammatory macrophages through an IL-10 receptor-JAK1/Tyk2/P-STAT3 associated pathway. Activation of M2 alternative macrophages exerting pro-fibrotic properties is dependent of the IL-4 and/or IL-13 signaling that respectively involve IL-4 receptor-JAK1/JAK3/P-STAT6 and IL-13 receptor-JAK1/JAK2/Tyk2/P-STAT6 associated pathways (16). JAK/STAT signaling are therefore key processes of macrophage polarization. By targeting specific pro-fibrotic pathways in macrophages, in addition with their impact on pro-inflammatory pathways, JAK inhibitors could therefore exert simultaneously anti-fibrotic and anti-inflammatory effects relying on their impact on macrophages. The effects of different JAK-inhibitors on the broad spectrum of activation of macrophages has however never been studied so far, especially considering pro-fibrotic macrophages. A systematic phenotypic and functional evaluation of the impact of different JAK inhibitors on the broad spectrum of activations states of macrophages is therefore mandatory. Moreover, there are conflicting results in the literature concerning *in vivo* effects of JAK inhibitors, as some studies report a switch from M1 to M2 activation after exposure to JAK3/JAK2 inhibitors such as tofacitinib (17) whereas a decrease of M2 polarization markers has been described after JAK2/1 inhibition by ruxolitinib (18). The precise impact of JAK inhibitors on a wide spectrum of activation states of macrophages is all the more important as the concept of a mutually exclusive M1/M2

polarization profile is more and more controverted, with a constant need of new relevant *in vivo* models to better approach this issue (19).

These potential unbalanced anti-inflammatory and anti-fibrotic properties of JAK inhibitors on macrophages could be especially important in the context of diseases characterized by concomitant inflammatory and fibrotic manifestations (20). Interstitial lung disease (ILD) and especially connective tissue disease/autoimmune disorders-associated ILD, are characterized by such combinations of pro-inflammatory and pro-fibrotic phenomena (20,21,22). ILD is a class of heterogeneous pulmonary disorders that involves the association of an infiltrate of mononuclear cells, especially including lung macrophages, with fibrotic features characterized by collagen depositions in the interstitial compartment and, in some cases, in the bronchial and/or alveolar lumen. ILD can have various origin, from acute ILD due to viral infections such as COVID-19 (23,24), to chronic ILD, for which autoimmune disorders are among the main causes. Although the potential therapeutic effects of some JAK inhibitors such as tofacitinib has been studied in a mouse model of pulmonary fibrosis (25,26), the effects of JAK2/1 inhibitors such as ruxolitinib on lung macrophages has never been studied so far. Moreover, the evaluation of the pulmonary effects of JAK inhibitors has especially focused on mouse models of ILD based on local / intratracheal challenging, such as the bleomycin mouse model (9), or on specific pro-autoimmune background (26). The potential therapeutic effects of JAK inhibitors on lung macrophages in the context of ILD with systemic trigger in wild-type mice have never been studied (27), particularly concerning scleroderma associated-ILD. Scleroderma (also called systemic sclerosis (SSc)) is an autoimmune fibrotic disease in which M1 and M2 macrophages play a key role both in the skin and the lung (20,28). The HOCl mouse model is a model of scleroderma associated-ILD based on the daily intradermal injection of HOCl (hypochlorous acid) in wild-type mice, without pro-autoimmune background. Daily

dermal injections of the pro-oxidative agent HOCl induce a systemic reaction that leads to the onset of the key clinical features of scleroderma, such as skin fibrosis and ILD (29).

In this study, we propose to directly compare the anti-inflammatory and anti-fibrotic effects of three JAK inhibitors (ruxolitinib (JAK2/1 inhibitor); tofacitinib (JAK3/2 inhibitor) and itacitinib (JAK1 inhibitor)) on 5 different activation states of primary human MDM *in vitro*. Based on these results, we also explore the effects of JAK2/1 inhibition on macrophages in the HOCl mouse model of scleroderma associated-ILD. This is an important issue since scleroderma is considered as the rheumatic disease with the highest individual mortality and morbidity. There is no disease-modifying drug approved so far for the treatment of systemic sclerosis (30, 31, 32). Specific targeting of key cytokines such as IL-6 (33) or single pathway such as the CTLA4 pathway have failed to reach their primary endpoints (34). Thus, Jakinibs through their effects on multiple cytokine receptors could be a relevant therapeutic option for systemic sclerosis/scleroderma.

2. Materials and Methods

2.1. Chemicals and reagents

Human recombinant cytokines IFN γ , IL-4, IL-13 and IL-10 were purchased from Peprotech (Neuilly sur Seine, France) and human recombinant M-CSF was obtained from Miltenyi Biotec SAS (Paris, France). Dexamethasone and Lipopolysaccharide (LPS) from E.coli (serotype: 055:B5) were purchased from Sigma-Aldrich (St-Quentin Fallavier, France). Ruxolitinib (JAK 2/1 inhibitor with IC₅₀ in cell-free medium for human JAK2 (2.8 nM) and for human JAK1 (3.3 nM) (35), tofacitinib (JAK3/2 inhibitor with IC₅₀ in cell free medium for human JAK3 (1.0 nM) and for human JAK2 (20.0 nM) (36) and itacitinib (JAK1 selective inhibitor with IC₅₀ in cell free medium for human JAK1 (2.0 nM) (37,38) were provided by MedChemTronica (Sollentuna, Sweden). Stock solutions of ruxolitinib, tofacitinib and

itacitinib were prepared in dimethyl sulfoxide (DMSO), whereas those of human recombinant cytokines were done in sterile distilled water containing 0.1% bovine serum albumin. Control cultures received the same dose of solvents as treated counterparts.

2.2. Preparation Monocyte-Derived Macrophages (MDM)

Peripheral blood mononuclear cells were obtained from blood buffy coats of healthy donors through Ficoll gradient centrifugation. Monocytes, selected after a 1-h adhesion step, were differentiated into MDM for 6 days using M-CSF (50 ng/ml) in RPMI 1640 medium GlutaMAX (Gibco, Life technologies SAS, Courtaboeuf, France) supplemented with antibiotics (20 IU/ml penicillin and 20 µg/ml streptomycin (ThermoFisher Scientific, Courtaboeuf, France)) and 10% heat-inactivated fetal bovine serum (FBS, Lonza, Levallois-Perret, France), as previously described (39). Blood buffy coats of healthy donors were provided by Etablissement Français du Sang (Rennes, France) and obtain after the written consent of all donors. This study was conducted in accordance with the declaration of Helsinki and was approved by our ethics committee/IRB (CPP Ile de France VI, project n°77-19 NI Cat. 3 ; 19.10.11.44241 ID RCB : 2019-A02611-56)

2.3. Treatment and polarization of MDM

At day 6, MDM were placed in medium with 5% of heat-inactivated FBS in the presence of M-CSF (10 ng/ml); this first state of differentiation corresponded to unpolarized M0-MDM. MDM were pre-treated for 1 h with 0.1 and 1 µM of ruxolitinib, tofacitinib, itacitinib or DMSO. For polarization, MDM were preserved in the same medium containing the inhibitors and activated for additional 20 h by the addition of 20 ng/ml IFN γ (M1i type), 20 ng/ml IFN γ and 20 ng/ml LPS (M1Li type), by the addition of 20 ng/ml IL-4 and 20 ng/ml IL-13 (M2a type), by 20 ng/ml IL-10 (M2c type) or by 20 ng/ml IL-10 with 10 nM of dexamethasone (M2c+dex

type). This method of *in vitro* polarization has been previously validated by our team (22). The effects of the JAK inhibitors were only considered if the polarizations were properly induced based on the polarization markers described in Fig. 1. At day 7, conditioned media were removed and stocked at -20°C for ELISA analysis whereas the cells were washed and harvested for RNA extraction or flow cytometry analysis.

2.4. Cell viability assay

The effects of JAK inhibitors on MDM cell viability were assessed using the tetrazolium salt WST-1 reagent. Briefly, 4-day differentiated MDM were seeded in 96-well plates at 1×10^5 cells/well to achieve their differentiation. Six day-old MDM were then exposed for 24 h to 0.1 or 1 μ M of ruxolitinib, tofacitinib, itacitinib or DMSO during polarization steps triggered as described above. MDM were then incubated with 10 μ l WST-1. The yellow formazan product formed by viable adherent cells after 1 h was further quantified by its absorbance at 450 nm using a SPECTROstar Nano spectrophotometer (BMG Labtech, Ortenberg, Germany).

2.5. Mouse model of HOCl-induced Systemic Sclerosis

Female C57BL/6J mice weighing between 18-20 gr, used at 8 weeks of age, were purchased from Janvier Labs (Le Genest Saint Isle, France). The animals were housed in positive pressure air-conditioned units (25°C, 50% relative humidity) on a 12-h light/dark cycle and were randomly divided into 3 groups: intradermal injections of PBS and oral solvent (0.5% Weight/Volume carboxymethyl glucose in NaCl 0.9% from Sigma-Aldrich (St-Quentin Fallavier, France)) (n=9), intradermal injections of HOCl and oral solvent (n=8, one loss due to biopsy sample at week 3), intradermal injections of HOCl and ruxolitinib (20 mg/kg, oral gavage twice a day) (n=9). The number of groups and mice per group was pre-calculated depending on statistical power considerations based on the expected results. This determination

of group size was performed in accordance with guidelines for animal experiments of the French government, with the objective to reduce the number of groups and mice per group to its minimum. Experimental scleroderma-associated ILD was induced by daily intradermal injections of 100 μ l of an HOCl-generating solution into each side of the shaved backs of mice (5 days a week) until week 3 and then of 200 μ l of the same solution in one side of the back for 3 more weeks (29). The HOCl-generating solution was daily prepared by adding NaClO solution (9.6% of active chlorine) to a 100 mM KH_2PO_4 solution (pH 6.2). The HOCl amount was determined through the evaluation of the optical density (OD) of the solution at 280 nm, and then adjusted to obtain an OD between 0.7 and 0.9. Control mice received 2 injections of 100 μ l of sterilized PBS as control. Animal studies were reviewed and approved by the Committee on the Ethics of Animal Experiments under the French Ministry of Higher Education and Research (permission#: 17011–2018100812449655 v3). The study was carried out in strict accordance with the recommendations in the Guide for the Care and Use of Laboratory Animals, EEC Council Directive 2010/63/EU.

2.6. Sample collection for in vivo experiments

After 3 weeks of experimental procedure, skin biopsies were performed using standardized biopsy punch near the HOCl-injection site at one side of the back of mice anesthetised with ketamine and xylazine (respectively 60 and 10 mg/kg). After 6 weeks of experimental procedure, mice were sacrificed with an overdose of ketamine and xylazine (respectively 100 and 20 mg/kg) and intracardiac exsanguination. Lungs were removed from each mouse, another skin sample was collected at the opposite site from the skin biopsy performed at week 3, and all samples were stored at -80°C until use, or fixed in 10% acetic acid formol for histopathological analyses.

2.7. *Histological analyses.*

Skin and lung samples embedded in paraffin were sliced into serial 4 μm sections. Sections were then stained using Masson's trichrome and picrosirius-red staining. Slides were then scanned with the NanoZoomer 2.0 RS (Hamamatsu, Tokyo, Japan). Images were captured for analysis using NDPview2 software (Hamamatsu). Skin thickness was evaluated by measuring the distance between the epidermal and the dermal–subcutaneous fat junction at a 10-fold magnification. Six random measurements per section were performed by a same blinded investigator and averaged for each section. Lung analyses were performed by a same investigator who was also blinded to the animal's group assignment.

2.8. *Hydroxyproline content in the lungs*

Collagen content in the lower lobe (left lung) was assessed using a colorimetric Hydroxyproline Kit Assay according to the manufacturer's protocol (BioVision, USA). Briefly, a lung piece of each mouse was homogenized in 500 μl of water and hydrolyzed at 120°C for 2 h in an equal volume of concentrated NaOH (10 M). The hydrolysate was secondly neutralized using equimolar adjunction of HCl (10 M). Then, a colorimetric product, visualized at 560 nm and proportional to the hydroxyproline content was generated using supplied reagents, based on an oxidization reaction, allowing the quantification of hydroxyproline in the entire lung lobe for each mouse (40).

2.9. *Reverse Transcription-quantitative Polymerase Chain Reaction (RT-qPCR) Experiments*

Total RNA were extracted from cells with Nucleospin RNA extraction Kit (Macherey-Nagel) and reverse transcribed using the High-Capacity cDNA Reverse Transcription Kit (Applied Biosystems, Thermo Fisher Scientific). qPCR assays were next performed using the fluorescent dye SYBR Green methodology and a CFX384 Real-Time PCR detector (Bio-Rad

Laboratories, Marnes-la-Coquette, France), as previously described (18). The KiCqStart® SYBR® Green primers for human and mouse cDNA were provided by Sigma-Aldrich. The specificity of amplified genes was evaluated using the comparative cycle threshold method (CFX Manager Software). These mean Cq values were used to normalize the target mRNA concentrations to those of the 18S ribosomal protein by the $2^{(-\Delta\Delta Cq)}$ method.

2.10. Quantification of cytokine and chemokine levels

Levels of IL-6, CXCL10, TNF α , CCL18 and PDGFbb secreted in culture media were quantified by ELISA using specific Duoset ELISA development system kits (R&D Systems : catalog numbers for IL-6: DY206 ; for CXCL10: DY266 ; for TNF α : DY210 ; for CCL18: DY394 ; and for PDGFbb: DY220). We have chosen to quantify these cytokines as they are specifically relevant for the pathogenesis of systemic sclerosis : serum level of IL-6, CXCL-10 and CCL-18 are elevated in the serum of patients with systemic sclerosis and their elevation is associated with more severe forms of the disease (41, 42, 43). PDGFbb is a key macrophagic marker that triggers fibroblast activation in SSc (44). TNF α is a key M1 marker that is widely used as a relevant pro-inflammatory polarisation marker (15).

2.11. Flow cytometry analyses

Phenotypic analysis of MDM was performed using flow cytometric direct immunofluorescence. After washing and plastic detachment using Accutase™ (BioLegends, Paris, France), cells were stained with Fixable Viability Stain 780 (BD Biosciences, Le Pont de Claix, France) for 10 min at room temperature to measure viability. MDM were first blocked in phosphate-buffered saline (PBS) supplemented with 2% FBS solution and with FcR blocking reagent (Miltenyi Biotec SAS, Paris, France) for 10 min at room temperature to avoid nonspecific binding, and then re-suspended and incubated with specific antibodies or

appropriate isotype controls for 30 min at 4°C. Cells were washed with PBS, collected by centrifugation (2500 rpm for 5 min) and then analyzed on a LSR II cytometer (BD Biosciences, San Jose, CA, USA) and FlowLogic™ software (Miltenyi Biotec SAS, Paris, France). The phenotypic characterization of MDM was performed using the following antibodies: BB515 anti-CD206 (ref 564668), BV421 anti-CD163 (ref 562643), BV605 anti-CD204 (ref 722440), BUV 395 anti-MHCII (ref 564040), APC anti-CD86 (ref 560956) and PE anti-TLR4 (ref 564215) and their respective isotype control, as recommended by BD Biosciences (Le Pont de Claix, France). Results are expressed as the mean ratio of median fluorescence intensity (MFI) calculated as follows: MFI (mAb of interest)/MFI (isotype control mAb).

2.12. Western blotting analyses

Protein extracts were prepared as previously described (21). Protein lysates were then separated on polyacrylamide gel and electrophoretically transferred onto Protan® nitrocellulose membranes (Whatman GmbH, Dassel, Germany). After blocking with Tris-buffered saline containing 4% (vol/vol) bovine serum albumin and 0.1% (vol/vol) Tween 20 for 30 min at room temperature, membranes were incubated overnight at 4 °C with primary antibodies against phospho-STAT1 (Tyr 701), phospho-STAT3 (Tyr 705), phospho-STAT6 (Tyr 641) and GAPDH from Cell Signaling Technology (Ozyme, Montigny-le Bretonneaux, France). After washing, membranes were next incubated with appropriate horseradish peroxidase-conjugated secondary antibodies (Dako, Glostrup, Denmark). Immunolabeled proteins were finally visualized by chemiluminescence. Densitometry with ImageJ 1.40 g software (National Institutes of Health, Bethesda, MD) was used for quantifying intensities of stained bands.

2.13. Statistical analyses

Data are presented as means \pm standard error on the mean (SEM). Comparison between more than 2 groups were performed by repeated measure analysis of variance for paired or one-way analysis of variance followed by Dunnett's or Newman-Keuls multiple comparison post-hoc tests for independent groups. Depending on conditions and Gaussian distribution, Student's *t* test, paired-t-test or Mann and Whitney test were used to compare 2 groups. A *P* value < 0.05 was considered significant. Data analyzes were performed with GraphPad Prism 5.0 software (GraphPad Software, La Jolla, CA, USA) and Heatmap (Fig. 6) was performed using Microsoft® Excel (V16.16.19).

3. Results

3.1. Validation of polarization markers and respective toxicity of considered JAK inhibitors for two concentrations relevant of human plasma levels

CXCL10, IL-6, IL1Ra and TNF α were all significantly over-expressed in the IFN γ -induced M1i MDM and in the (IFN γ +LPS)-induced M1Li MDM (Fig. 1A-B) in comparison with M0 unstimulated MDM. CCL18, PDGFbb, PPAR γ and tenascin C (TenaC) were significantly over-expressed in the (IL-4/IL-13)-induced M2a MDM in comparison with M0 unstimulated MDM (Fig. 1C-D). CXCL13, IL-10, MARCO and SOCS3 were all upregulated in the IL-10-induced M2c MDM and in the (IL-10/Dexamethasone)-induced M2c+Dex (Fig. 1E). Considering phenotype, CD86 were upregulated in M1i and M1Li MDM, TLR4 in M1i and MHCII in M1Li, in comparison with M0 and with all M2 MDM (Fig. 1F). CD206 was confirmed as a M2a marker in our model of MDM, CD163 as a M2c marker in comparison with M1Li and CD204 as a marker of M2c+dex polarization (Fig. 1F). Treatment of unpolarised M0 or polarized MDM by 0.1 and 1 μ M of ruxolitinib for 24 h did not trigger toxicity (Fig. 2A). Tofacitinib had no significant impact on cell viability for both concentrations in M0, M1i,

M1Li and M2a, but showed significant cell toxicity in M2c and M2c+dex MDM at 1 μ M but not at 0.1 μ M; the same results were observed for itacitinib in M2c+dex. The detailed results of the effect of JAK inhibitors are therefore presented at 1 μ M for M1i/Li and M2a MDM, and at 1 μ M and 0.1 μ M for M2c and M2c+dex MDM. Nonetheless, the impact of all three JAK inhibitors on the key polarization markers in all polarization states at 1 μ M and 0.1 μ M are summarized in Fig. 6.

3.2. JAK inhibitors limited the pro-inflammatory activation of macrophages, in two M1 MDM models with more pronounced effects of the JAK2 inhibitors.

In M1i MDM, a pre-treatment by the 3 JAK inhibitors (1 h at 1 μ M before activation) limited mRNA expressions of key inflammatory cytokines associated with M1i polarization induced by IFN γ (CXCL10, IL-6, TNF α) (Fig. 3A); the effects of ruxolitinib was more significant on these cytokines than those of the two other JAK inhibitors (difference between itacitinib and ruxolitinib for the down-regulation of CXCL10: $p < 0.001$; difference between both itacitinib/tofacitinib and ruxolitinib for the down-regulation of TNF α : $p < 0.05$ for both), and only ruxolitinib had an effect on the mRNA expression of IL1Ra ($p < 0.05$). Fold changes are summarized in Figure 6. In M1Li, JAK inhibitors reduced efficiently the mRNA expression of CXCL10, TNF α , and IL1ra, with once again a more prominent effect of ruxolitinib, especially in comparison with itacitinib (differences between ruxolitinib and itacitinib: $p < 0.001$ for CXCL10, $p < 0.001$ for IL-1 Ra, $p < 0.05$ for TNF α ; differences between ruxolitinib and tofacitinib: $p < 0.05$ for CXCL10 and $p < 0.05$ for IL1-Ra) (Fig. 3B). JAK inhibitors partly reduced the mRNA expression of IL-6 in this M1Li polarization state, without however reaching a significant level. At the protein level, JAK inhibitors tended to reduce the secretion of CXCL10 and IL-6 in M1i MDM, but without reaching statistical significance (Fig. 3C). Only ruxolitinib significantly reduced the secretion of TNF α by M1i MDM ($p < 0.05$) (Fig. 3C). In

M1Li MDM, all three JAK inhibitors reduced significantly the secretion of IL-6, itacitinib had no significant effect on CXCL10 secretion, and only ruxolitinib significantly reduced TNF α secretion levels (Fig. 1D). From a phenotypic viewpoint, all JAK inhibitors reduced the expression of the IFN γ -induced markers CD86 and TLR4 with a more important effect of ruxolitinib (Fig. 1E). Only ruxolitinib and tofacitinib limited the upregulation of MHCII in M1i MDM, with a more pronounced effect of ruxolitinib ($p < 0.001$ for ruxolitinib in comparison with untreated M1i; $p < 0.05$ for tofacitinib in comparison with untreated M1i). In M1Li MDM, only ruxolitinib significantly reduced CD86 expression ($p < 0.01$ in comparison with untreated M1i) (Fig. 1F) and tended to reduce the expression of MHCII (Fig. 1F).

3.3. JAK inhibitors limited the expression of key secreted and phenotypic markers of alternative macrophages, in three M2 MDM models.

A pre-treatment by the different JAK inhibitors (1 h at 1 μ M before activation) limited the mRNA expression of key polarization markers induced by M2a polarization. Thus, mRNA expressions of CCL18, PDGFbb, PPAR γ were significantly reduced by the three JAK inhibitors, with a more pronounced effect of tofacitinib on PPAR γ (Fig. 4A). Only ruxolitinib significantly reduced the M2a marker TenaC ($p < 0.05$ in comparison with untreated M2a). In term of secretion, the CCL18 levels in M2a MDM were similarly reduced by all three inhibitors (Fig. 4B). PDGFbb tended to be down-secreted by M2a MDM exposed to ruxolitinib only (Fig. 4B). The membrane expression of CD206 was significantly reduced by all JAK inhibitors (Fig. 4C). Fold changes are summarized in Figure 6.

In IL-10-induced M2c and in (IL10+dexamethasone)-induced M2c+dex MDM, mRNA expressions of CXCL13, MARCO and SOCS3 were down-regulated by all JAK inhibitors used at 1 μ M, with a more pronounced effect of ruxolitinib on SOCS3 transcripts (comparison between ruxolitinib and itacitinib, $p < 0.01$; comparison between tofacitinib and itacitinib,

$p < 0.05$) (Fig. 5A and E). Membrane expression of CD163 was only significantly reduced by itacitinib in M2c MDM ($p < 0.05$) (Fig. 5B), whereas the membrane expression of CD204 was unchanged in M2c+dex for all JAK inhibitors (Fig. 5F). Considering the impact of tofacitinib and itacitinib on MDM viability in M2c and M2c+dex respectively, we also presented the detailed results for treatments at 0.1 μM . At this concentration, all JAK inhibitors reduced the mRNA expression of SOCS3, with a more significant effect of ruxolitinib (Fig. 5C). The mRNA expression of MARCO in M2c+dex was also reduced by ruxolitinib, with no significant effect of tofacitinib and itacitinib (Fig. 5G). At 0.1 μM , JAK inhibitors had no impact on the phenotype of M2c and M2c+dex MDM (Fig. 5D and H). Fold changes are also summarized in Figure 6.

3.4. The JAK2/JAK1 inhibitor ruxolitinib reduced the phosphorylation of STAT proteins induced in polarized MDM

The impact of these 3 JAK inhibitors at the concentration of 1 and 0.1 μM on the key polarization markers of the 5 models of polarized MDM are summarized in Fig. 6. Considering that, in these 5 polarization states, ruxolitinib was the JAK inhibitor with the more pronounced effects both at 1 and 0.1 μM , we selected this JAK2/1 inhibitor to confirm its capacity to limit the phosphorylation of key STAT proteins. Thus, a pre-treatment by ruxolitinib significantly reduced the phosphorylation of STAT-1 in M1i and M1Li MDM (Fig. 7A), STAT-6 in M2a MDM (Fig. 7B) and STAT-3 in the two models of M2c MDM (Fig. 7C).

3.5 Ruxolitinib prevented the development of ILD in a mouse model of scleroderma, and significantly reduced the expression of key polarization markers of both M1 and M2 macrophages.

This mouse model of scleroderma-associated ILD is based on a daily intradermal injection of HOCl, leading to cutaneous inflammation and fibrosis, with subsequent systemic inflammation and autoimmunity, leading to visceral involvement, especially in the lung (ILD) (29). In accordance with the clinical biological features of the human scleroderma autoimmune disease (20), these HOCl injections upregulated the mRNA expression of key macrophagic M1 ($\text{TNF}\alpha$, CXCL10, NOS2) and M2 (Arg1) markers in the skin (Fig. 8A-B).

The skin mRNA induction for M1 markers was especially significant after 3 weeks of injections but not after 6 weeks. On the contrary, the mRNA expression of the M2 marker Arg1 was only significantly induced after 6 weeks; a trend towards an upregulation was observed at 3 weeks for the M2 marker CHI3L3, but with high variability of expression between mice (Fig. 8A-B). These results stressed the relevance of targeting both M1 and M2 macrophages throughout the disease process, with a specific importance of an early targeting of M1 macrophages. In accordance with this hypothesis, the treatment by ruxolitinib, significantly repressed the expression of M1 markers (CXCL10, NOS2) after 3 weeks (Fig. 8A), and M2 markers (Arg1, Chi3L3) after 6 weeks of injection (Fig. 8B). Considering histological outcomes, after 6 weeks of intradermal injections, dermal thickness was significantly upregulated in the HOCl group in comparison with the control saline injected group, and ruxolitinib significantly reduced this dermal effect of HOCl (Fig. 8C to F).

We secondly explored the effects of ruxolitinib on pulmonary involvement, as it is the deadliest manifestation of scleroderma in human (32). Daily intradermal injections of HOCl induced a pulmonary reaction characterized by a widespread ILD, involving sub-pleural, intraparenchymal and peri-bronchial regions (Fig. 9A). This pulmonary involvement was especially pronounced in sub-pleural region (Fig.9E), similarly to the scleroderma-associated ILD in human (45). In accordance with previous studies based on this model, this pulmonary involvement was characterized by marked collagen deposits as observed by Sirius red staining

(Fig. 9B), hydroxyproline content (Fig. 9C) and mRNA upregulation of profibrotic genes (Acta2, Fn1, TGFb1, Col1A1, Col3A1)(Fig. 9D). When focusing on macrophages, HOCl injections induced a pulmonary infiltrate of mononuclear cells, especially in sub-pleural regions (Fig. 9E), with a concomitant mRNA upregulation of both key macrophagic M1 markers (IL-6, TNF α , CXCL10, Ifi44, NOS2) and key M2 markers (Arg1, Retnla, Chi3L3, Flt1, IL4Ra) (Fig. 9F). Treatment by ruxolitinib significantly reduced HOCl-induced ILD, as reflected by a significant reduction of profibrotic marker expression and of hydroxyproline content (Fig. 9C and D). Moreover, ruxolitinib significantly prevented the upregulation of pro-inflammatory M1 markers (TNF α , CXCL10, IFi44, NOS2) and pro-fibrotic M2 markers (Arg1, Retnla, Chi3L3, Flt1, IL4Ra), concomitantly with a reduction of mononuclear pulmonary infiltrate (Fig. 9E-F).

4. Discussion

Prior studies from our team have highlighted that JAK2/1 inhibition by ruxolitinib could limit pro-inflammatory properties of LPS activated MDM *in vitro* (14), notably through a down-regulation of interferon β (IFN β) signature and IL-6 expression. Our study goes further through the direct comparison of the impact of three JAK inhibitors on a wide spectrum of activation states in primary human M-CSF-derived MDM. We highlight that Jakinibs with inhibitory properties over JAK2 (mostly ruxolitinib and to lesser extent, tofacitinib) in comparison with JAK1 inhibition by itacitinib, can more significantly limit the expression of pro-inflammatory markers as well as pro-fibrotic markers in a dose-dependent manner. It is noteworthy that the *in vitro* active concentration of 1 μ M is in the range of plasmatic levels of JAK inhibitors in human patients under a normal regimen (46, 47, 48, 49). Moreover, the proposed concentrations of 1 and 0.1 μ M are in line with previous studies evaluating the effects on these JAK inhibitors on various cell types *in vitro* (50,51). Furthermore, in a mouse model of systemic sclerosis, a pro-inflammatory and pro-fibrotic disease characterized by a

simultaneous over-activation of both M1 and M2 macrophages, we confirm the inhibitory effects of ruxolitinib on the expression of key M1 and M2 markers in the lung and skin. Although the impact of ruxolitinib and tofacitinib on skin fibrosis has already been recently explored in a mouse model of bleomycin-induced skin fibrosis (27), the impact of JAK2/1 inhibition by ruxolitinib in a mouse model of ILD with systemic trigger was still to be determined. This is a topical issue, since tofacitinib is evaluated in clinical phase I/II trials for systemic sclerosis (52). In case of disappointed clinical results, further results on pre-clinical models, such as those presented in our work, comparing different JAK inhibitors and supporting the preferential use of some of them will be of great interest to select possible more relevant candidate drugs (53).

The overall superiority of Jakinibs with inhibitory properties over JAK2 (mostly ruxolitinib and to lesser extent, tofacitinib) on all polarization states in comparison with itacitinib is in accordance with the signaling pathways involved in macrophage polarization. JAK2 is involved in IL-13 and IFN γ signaling, ruxolitinib through its combined effect on JAK1 and JAK2, could largely suppressed IFN γ signaling and IL-13 signaling pathways, with a direct impact both on M1 and M2a polarization. Although tofacitinib is a first-in-class JAK3 inhibitor, it shows limited selectivity for JAK1 and 2 (54,55). Through its effect on JAK2 tofacitinib can thus also impact IFN γ signaling and IL-13 signaling pathways and by implication the M1 and M2a polarization. The more selective inhibition of JAK1 by itacitinib could explain its more pronounced impact on the IL-10-induced M2c marker CD163. Nonetheless, this impact was only observed at 1 μ M. Moreover, this more pronounced effect of itacitinib was not observed for other M2c markers such as SOCS3 or MARCO, for which ruxolitinib had the most down-regulating effect. Itacitinib may nonetheless appear relevant for fibrotic disorders characterized by milder inflammation and especially those including macrophages and IL-10 signaling, such as idiopathic pulmonary fibrosis (IPF) (56). On the contrary, JAK2/1 inhibition by ruxolitinib

and baricitinib has been proposed as a candidate strategy to target highly inflammatory ILD, characterized by a pro-inflammatory cytokine burst. This is for example the case for COVID-19-associated ILD (23,24), in which a high concentration of the M1 cytokine CXCL10 is found in bronchoalveolar lavage (BAL) fluids of patients infected by SARS-CoV-2 (57). The strong repression of CXCL10 expression by ruxolitinib in our model of MDM and in our *in vivo* model supports such hypothesis.

The HOC1-induced systemic sclerosis-associated ILD model was especially relevant to test our hypothesis of a widespread impact of JAK2/1 inhibition on various activation states of macrophages because an upregulation of the phosphorylation of STAT3 and STAT6 was previously observed in this *in vivo* model (58,59). Moreover, monocytes from scleroderma patients have an upregulated IFN signature, especially including the STAT1 signaling pathway (60). This mouse model was also of interest since ILD in HOC1 mice is associated with an infiltrate of lung macrophages, as previously demonstrated (61). Nonetheless, so far, the polarization profile of lung macrophages in this model had never been characterized and the impact on therapeutic agents on the activation states of lung macrophages had never been evaluated in this model. In our study, we demonstrate that, similarly to what has been observed in the skin of patients with systemic sclerosis (20), the mRNA expression of both M1 (TNF α , CXCL10, Ifi44, NOS2) and M2 (Arg1, Retnla, Chi3L3, Flt1, IL4Ra) markers were upregulated in this mice model of ILD. In accordance with our *in vitro* results in human MDM, ruxolitinib could significantly balance this upregulation, resulting in the return of all gene expressions to a normal range, although Arg1 expression even tended to be down-regulated in comparison with control. Some of M1 markers that we studied in human MDM and that were down-regulated by ruxolitinib could be directly transposed to mouse macrophages, such as CXCL10 or TNF α , with similar results concerning the impact of JAK2/1 inhibition in the two species. Nonetheless, other key polarization markers are not shared among the two species and among different

tissues (62) and we therefore selected genes that were especially relevant in mouse for our *in vivo* experiments (63). Expectedly, the upregulation of M1 and M2 markers in HOCl group was associated with upregulation of fibrotic markers, as HOCl-ILD model associates inflammatory and fibrotic disorder. Beyond impacting the polarization profile of macrophages in this model, ruxolitinib also reduced fibrotic markers and lung hydroxyproline content. We cannot exclude that this anti-fibrotic effects of ruxolitinib is the consequence of its direct effect on fibroblasts, as previously suggested for localized lung fibrosis induced by intratracheal instillation of bleomycin (9). Thus, the central role of macrophages in the pathogenesis of ILD is also supported by experiments demonstrating that the specific genetic deletion of monocyte-derived alveolar macrophages after their recruitment to the lung ameliorates lung fibrosis (64). Systemic sclerosis is a disease also including pure inflammatory manifestations, such as inflammatory articular phenomenon (65), that are not driven by fibroblasts. Therefore, the identification of other cellular targets in experimental models of this disease is of primary importance and our results support the hypothesis that the activation states of macrophages are considerably impacted in this disease (66).

There are several limitations in our study. First, the use of M-CSF-derived blood MDM as a model of tissue macrophages could be considered as a weakness of our study, as we did not directly use macrophages from BAL of patients with systemic sclerosis. Nonetheless we have previously demonstrated that M-CSF-derived blood MDM shared phenotypic and activation properties of lung macrophages from BAL of patients with ILD such as sarcoidosis-associated ILD but also, and most importantly, systemic sclerosis-associated ILD (39). Furthermore, it has been recently demonstrated that MDM from patients with systemic sclerosis shared common activation states with skin macrophages from biopsy samples from the same patients (67). Second, we only evaluated the impact of ruxolitinib on one mouse model of systemic sclerosis. Nonetheless, HOCl-induced scleroderma-associated ILD, could be

considered as one of the best models to evaluate macrophage polarization considering the over-expression of key P-STAT and, also considering that it is a systemic form of the disease and not a localized induced lung fibrosis, contrarily to the intratracheal bleomycin model. Moreover, our *in vivo* experiments are only preventive studies, interventional studies would have been more clinically relevant. Another limitation is that we did not performed a direct *in vivo* comparison of the effects of ruxolitinib and tofacitinib on ILD, which would have been relevant to specifically precise the respective impact of JAK2 and JAK3 inhibition in our mouse model. This comparison would also have helped to strengthen the relevance of the differences observed *in vitro*, considering that the IC50 for JAK2 is different by 10-fold between ruxolitinib and tofacitinib (38,55). Testing the hypothesis of an overall superiority of ruxolitinib over tofacitinib at a dose that would have comparable effects to inhibit JAK2 would have helped to highlight which jakinibs could be the most relevant for systemic sclerosis-associated ILD, and how much important JAK3 is for the pathogenesis of this disease (considering equal inhibition of JAK2). Another limitation of our study is that we only focused on macrophages, specifically considering their relevance in the pathogenesis of systemic sclerosis. Beyond macrophages, recent studies have demonstrated that JAK inhibitors such as tofacitinib could suppressed the progression of ILD in a mouse model of rheumatoid arthritis-associated ILD. These effects of tofacitinib were specifically mediated by an expansion of myeloid-derived suppressor cells, which are immature myeloid cells with a suppressive function that negatively control inflammation, notably in the lung. Their relevance in systemic sclerosis is still to be determined, but they could also play a role in the impact of ruxolitinib on the HOC1-mouse model (26).

Overall, our results suggest that the combined anti-inflammatory and anti-fibrotic properties of JAK2 inhibitors could be relevant to target lung macrophages in autoimmune and inflammatory pulmonary disorders that have no efficient disease modifying drugs to date. Our results emphasizes the impact of JAK inhibitors on the polarization states of skin and lung

macrophages. Beyond the issue of polarization profile, the impact of JAK inhibitors on the functional resolving properties of macrophages may also represent a relevant issue for the treatment of pulmonary and systemic disorders and this question may deserves dedicated studies in the future (1,2,28, 68).

CRedit authorship contribution statement

Alain Lescoat: Conceptualization, Validation, Formal analysis, Investigation, Writing, Visualization, Funding acquisition. **Marie Lelong:** Validation, Investigation. **Mohamed Jeljeli:** Methodology, Resources. **Claire Piquet-Pellorce:** Investigation, Methodology. **Claudie Morzadec:** Investigation, Resources. **Alice Ballerie:** Writing, Visualization, Funding acquisition. **Stéphane Jouneau:** Writing, Visualization, Funding acquisition. **Patrick Jégo:** Resources, Funding acquisition. **Laurent Vernhet:** Resources, Conceptualization, Writing. **Frédéric Batteux:** Methodology, Resources. **Olivier Fardel:** Conceptualization, Writing, Funding acquisition. **Valérie Lecureur:** Conceptualization, Validation, Formal analysis, Investigation, Writing, Supervision, Funding acquisition.

Acknowledgements

The authors thank the animal house facilities (ARCHE), the platform of Flow cytometry and the Platform of Histo-Pathology High Precision (H₂P₂) (Biosit, Rennes, France). We would also like to thank N. Gouault (Institut des sciences chimiques de Rennes) for giving us access to the oven required to quantify hydroxyproline and N. Belhomme for helpful comments and critically reading the manuscript. This work was supported by the Institut National de la Santé et de la Recherche Médicale (INSERM), the Université de Rennes (Univ Rennes) and the “Association des sclérodermiques de France”.

References

- 1- Gadina M, Chisolm DA, Philips RL, McInness IB, Changelian PS, O'Shea JJ. Translating JAKs to Jakinibs. *J Immunol.* 2020 Apr 15;204(8):2011-2020.
- 2- Gadina M, Le MT, Schwartz DM, Silvennoinen O, Nakayamada S, Yamaoka K, O'Shea JJ. Janus kinases to jakinibs: from basic insights to clinical practice. *Rheumatology (Oxford).* 2019 Feb 1;58(Suppl 1):i4-i16.
- 3-Verstovsek S, Kantarjian H, Mesa RA, Pardanani AD, Cortes-Franco J, Thomas DA, Estrov Z, Fridman JS, Bradley EC, Erickson-Viitanen S, Vaddi K, Levy R, Tefferi A. Safety and efficacy of INCB018424, a JAK1 and JAK2 inhibitor, in myelofibrosis. *N Engl J Med.* 2010 Sep 16;363(12):1117-27.
- 4-Taylor PC, Keystone EC, van der Heijde D, Weinblatt ME, Del Carmen Morales L, Reyes Gonzaga J, Yakushin S, Ishii T, Emoto K, Beattie S, Arora V, Gaich C, Rooney T, Schlichting D, Macias WL, de Bono S, Tanaka Y. Baricitinib versus Placebo or Adalimumab in Rheumatoid Arthritis. *N Engl J Med.* 2017 Feb 16;376(7):652-662.
- 5-Fleischmann R, Kremer J, Cush J, Schulze-Koops H, Connell CA, Bradley JD, Gruben D, Wallenstein GV, Zwillich SH, Kanik KS; ORAL Solo Investigators. Placebo-controlled trial of tofacitinib monotherapy in rheumatoid arthritis. *N Engl J Med.* 2012 Aug 9;367(6):495-507.
- 6-Meyer DM, Jesson MI, Li X, Elrick MM, Funckes-Shippy CL, Warner JD, Gross CJ, Dowty ME, Ramaiah SK, Hirsch JL, Saabye MJ, Barks JL, Kishore N, Morris DL. Anti-inflammatory activity and neutrophil reductions mediated by the JAK1/JAK3 inhibitor, CP-690,550, in rat adjuvant-induced arthritis. *J Inflamm (Lond).* 2010 Aug 11;7:41.
- 7-Keystone EC, Taylor PC, Drescher E, Schlichting DE, Beattie SD, Berclaz PY, Lee CH, Fidelus-Gort RK, Luchi ME, Rooney TP, Macias WL, Genovese MC. Safety and efficacy of baricitinib at 24 weeks in patients with rheumatoid arthritis who have had an inadequate response to methotrexate. *Ann Rheum Dis.* 2015 Feb;74(2):333-40.
- 8-Wang H, Feng X, Han P, Lei Y, Xia Y, Tian D, Yan W. The JAK inhibitor tofacitinib ameliorates immune-mediated liver injury in mice. *Mol Med Rep.* 2019 Dec;20(6):4883-4892
- 9-Zhang Y, Liang R, Chen CW, Mallano T, Dees C, Distler A, Reich A, Bergmann C, Ramming A, Gelse K, Mielenz D, Distler O, Schett G, Distler JHW. JAK1-dependent transphosphorylation of JAK2 limits the anti-fibrotic effects of selective JAK2 inhibitors on long-term treatment. *Ann Rheum Dis.* 2017 Aug;76(8):1467-1475.

- 10-Al-Fayoumi S, Hashiguchi T, Shirakata Y, Mascarenhas J, Singer JW. Pilot study of the anti-fibrotic effects of the multikinase inhibitor pacritinib in a mouse model of liver fibrosis. *J Exp Pharmacol*. 2018 May 9;10:9-17.
- 11-Oh RS, Haak AJ, Smith KMJ, Ligresti G, Choi KM, Xie T, Wang S, Walters PR, Thompson MA, Freeman MR, Manlove LJ, Chu VM, Feghali-Bostwick C, Roden AC, Schymeinsky J, Pabelick CM, Prakash YS, Vassallo R, Tschumperlin DJ. RNAi screening identifies a mechanosensitive ROCK-JAK2-STAT3 network central to myofibroblast activation. *J Cell Sci*. 2018 May 15;131(10).
- 12-You H, Xu D, Zhao J, Li J, Wang Q, Tian X, Li M, Zeng X. JAK Inhibitors: Prospects in Connective Tissue Diseases. *Clin Rev Allergy Immunol*. 2020 Mar 28.
- 13-Goll GL, Kvien TK. New-generation JAK inhibitors: how selective can they be? *Lancet*. 2018 Jun 23;391(10139):2477-2478.
- 14-Febvre-James M, Lecureur V, Augagneur Y, Mayati A, Fardel O. Repression of interferon β -regulated cytokines by the JAK1/2 inhibitor ruxolitinib in inflammatory human macrophages. *Int Immunopharmacol*. 2018 Jan; 54:354-365.
- 15-Murray PJ, Wynn TA. Protective and pathogenic functions of macrophage subsets. *Nat Rev Immunol*. 2011 Oct 14;11(11):723-37.
- 16- Martinez FO, Gordon S. The M1 and M2 paradigm of macrophage activation: time for reassessment. *F1000Prime Rep*. 2014 Mar 3;6:13.
- 17-De Vries LCS, Duarte JM, De Krijger M, Welting O, Van Hamersveld PHP, Van Leeuwen-Hilbers FWM, Moerland PD, Jongejan A, D'Haens GR, De Jonge WJ, Wildenberg ME. A JAK1 Selective Kinase Inhibitor and Tofacitinib Affect Macrophage Activation and Function. *Inflamm Bowel Dis*. 2019 Mar 14;25(4):647-660.
- 18-Chen H, Li M, Sanchez E, Soof CM, Bujarski S, Ng N, Cao J, Hekmati T, Zahab B, Nosrati JD, Wen M, Wang CS, Tang G, Xu N, Spektor TM, Berenson JR. JAK1/2 pathway inhibition suppresses M2 polarization and overcomes resistance of myeloma to lenalidomide by reducing TRIB1, MUC1, CD44, CXCL12, and CXCR4 expression. *Br J Haematol*. 2020 Jan;188(2):283-294.
- 19-Murray PJ. Macrophage Polarization. *Annu Rev Physiol*. 2017 Feb 10;79:541-566.
- 20-Skaug B, Khanna D, Swindell WR, Hinchcliff ME, Frech TM, Steen VD, Hant FN, Gordon JK, Shah AA, Zhu L, Zheng WJ, Browning JL, Barron AMS, Wu M, Visvanathan S, Baum P, Franks JM, Whitfield ML, Shanmugam VK, Domsic RT, Castelino FV, Bernstein EJ, Wareing N, Lyons MA, Ying J, Charles J, Mayes MD, Assassi S. Global skin gene

- expression analysis of early diffuse cutaneous systemic sclerosis shows a prominent innate and adaptive inflammatory profile. *Ann Rheum Dis.* 2020 Mar;79(3):379-386.
- 21-Bellamri N, Viel R, Morzadec C, Lecureur V, Joannes A, de Latour B, Llamas-Gutierrez F, Wollin L, Jouneau S, Vernhet L. TNF- α and IL-10 Control CXCL13 Expression in Human Macrophages. *J Immunol.* 2020 Mar 25.
- 22-Lescoat A, Ballerie A, Jouneau S, Fardel O, Vernhet L, Jégo P, Lecureur V. M1/M2 polarisation state of M-CSF blood-derived macrophages in systemic sclerosis. *Ann Rheum Dis.* 2019 Nov;78(11):e127.
- 23-Zhang W, Zhao Y, Zhang F, Wang Q, Li T, Liu Z, Wang J, Qin Y, Zhang X, Yan X, Zeng X, Zhang S. The use of anti-inflammatory drugs in the treatment of people with severe coronavirus disease 2019 (COVID-19): The Perspectives of clinical immunologists from China. *Clin Immunol.* 2020 Mar 25;214:108393.
- 24-Richardson P, Griffin I, Tucker C, Smith D, Oechsle O, Phelan A, Stebbing J. Baricitinib as potential treatment for 2019-nCoV acute respiratory disease. *Lancet.* 2020 Feb 15;395(10223):e30-e31.
- 25-Wang W, Bhattacharyya S, Marangoni RG, Carns M, Dennis-Aren K, Yeldandi A, Wei J, Varga J. The JAK/STAT pathway is activated in systemic sclerosis and is effectively targeted by tofacitinib, *Journal of Scleroderma and Related Disorders*, 2019 Aug; 5(1):40–50.
- 26-Sendo S, Saegusa J, Yamada H, Nishimura K, Morinobu A. Tofacitinib facilitates the expansion of myeloid-derived suppressor cells and ameliorates interstitial lung disease in SKG mice. *Arthritis Res Ther.* 2019 Aug 6;21(1):184.
- 27-Damsky W, Patel D, Garelli CJ, Garg M, Wang A, Dresser K, Deng A, Harris JE, Richmond J, King B. Jak Inhibition Prevents Bleomycin-Induced Fibrosis in Mice and Is Effective in Patients with Morphea. *J Invest Dermatol.* 2020 Jan 16.
- 28-Ballerie A, Lescoat A, Augagneur Y, Lelong M, Morzadec C, Cazalets C, Jouneau S, Fardel O, Vernhet L, Jégo P, Lecureur V. Efferocytosis capacities of blood monocyte-derived macrophages in systemic sclerosis. *Immunol Cell Biol.* 2019 Mar;97(3):340-347.
- 29-Servettaz A, Goulvestre C, Kavian N, Nicco C, Guilpain P, Chéreau C, Vuiblet V, Guillevin L, Mouthon L, Weill B, Batteux F. Selective oxidation of DNA topoisomerase 1 induces systemic sclerosis in the mouse. *J Immunol.* 2009 May 1;182(9):5855-64.
- 30-The Lancet. Systemic sclerosis: advances and prospects. *Lancet.* 2017 Oct 7;390(10103):1624.

- 31-Distler O, Highland KB, Gahlemann M, Azuma A, Fischer A, Mayes MD, Raghu G, Sauter W, Girard M, Alves M, Clerisme-Beaty E, Stowasser S, Tetzlaff K, Kuwana M, Maher TM; SENSICIS Trial Investigators. Nintedanib for Systemic Sclerosis-Associated Interstitial Lung Disease. *N Engl J Med*. 2019 Jun 27;380(26):2518-2528.
- 32-Denton CP, Khanna D. Systemic sclerosis. *Lancet*. 2017 Oct 7;390(10103):1685-1699.
- 33-Khanna D, Denton CP, Jahreis A, van Laar JM, Frech TM, Anderson ME, Baron M, Chung L, Fierlbeck G, Lakshminarayanan S, Allanore Y, Pope JE, Riemekasten G, Steen V, Müller-Ladner U, Lafyatis R, Stifano G, Spotswood H, Chen-Harris H, Dziadek S, Morimoto A, Sornasse T, Siegel J, Furst DE. Safety and efficacy of subcutaneous tocilizumab in adults with systemic sclerosis (faSScinate): a phase 2, randomised, controlled trial. *Lancet*. 2016 Jun 25;387(10038):2630-2640.
- 34-Khanna D, Spino C, Johnson S, Chung L, Whitfield ML, Denton CP, Berrocal V, Franks J, Mehta B, Molitor J, Steen VD, Lafyatis R, Simms RW, Gill A, Kafaja S, Frech TM, Hsu V, Domsic RT, Pope JE, Gordon JK, Mayes MD, Schioppa E, Young A, Sandorfi N, Park J, Hant FN, Bernstein EJ, Chatterjee S, Castellino FV, Ajam A, Wang Y, Wood T, Allanore Y, Matucci-Cerinic M, Distler O, Singer O, Bush E, Fox DA, Furst DE. Abatacept in Early Diffuse Cutaneous Systemic Sclerosis: Results of a Phase II Investigator-Initiated, Multicenter, Double-Blind, Randomized, Placebo-Controlled Trial. *Arthritis Rheumatol*. 2020 Jan;72(1):125-136.
- 35-Quintás-Cardama A, Vaddi K, Liu P, Manshour T, Li J, Scherle PA, Caulder E, Wen X, Li Y, Waeltz P, Rupar M, Burn T, Lo Y, Kelley J, Covington M, Shepard S, Rodgers JD, Haley P, Kantarjian H, Fridman JS, Verstovsek S. Preclinical characterization of the selective JAK1/2 inhibitor INCB018424: therapeutic implications for the treatment of myeloproliferative neoplasms. *Blood*. 2010 Apr 15;115(15):3109-17.
- 36-Jiang JK, Ghoreschi K, Deflorian F, Chen Z, Perreira M, Pesu M, Smith J, Nguyen DT, Liu EH, Leister W, Costanzi S, O'Shea JJ, Thomas CJ. Examining the chirality, conformation and selective kinase inhibition of 3-((3R,4R)-4-methyl-3-(methyl(7H-pyrrolo[2,3-d]pyrimidin-4-yl)amino)piperidin-1-yl)-3-oxopropanenitrile (CP-690,550). *J Med Chem*. 2008 Dec 25;51(24):8012-8.
- 37-Mascarenhas JO, Talpaz M, Gupta V, Foltz LM, Savona MR, Paquette R, Turner AR, Coughlin P, Winton E, Burn TC, O'Neill P, Clark J, Hunter D, Assad A, Hoffman R, Verstovsek S. Primary analysis of a phase II open-label trial of INCB039110, a selective JAK1 inhibitor, in patients with myelofibrosis. *Haematologica*. 2017 Feb;102(2):327-335.
- 38-Kettle JG, Åstrand A, Catley M, Grimster NP, Nilsson M, Su Q, Woessner R. Inhibitors of JAK-family kinases: an update on the patent literature 2013-2015, part 1. *Expert Opin Ther Pat*. 2017 Feb;27(2):127-143.

- 39-Lescoat A, Ballerie A, Augagneur Y, Morzadec C, Vernhet L, Fardel O, Jégo P, Jouneau S, Lecreur V. Distinct Properties of Human M-CSF and GM-CSF Monocyte-Derived Macrophages to Simulate Pathological Lung Conditions In Vitro: Application to Systemic and Inflammatory Disorders with Pulmonary Involvement. *Int J Mol Sci*. 2018 Mar 17;19(3).
- 40-Kavian N, Mehlal S, Jeljeli M, Saidu NEB, Nicco C, Cerles O, Chouzenoux S, Cauvet A, Camus C, Ait-Djoudi M, Chéreau C, Kerdine-Römer S, Allanore Y, Batteux F. The Nrf2-Antioxidant Response Element Signaling Pathway Controls Fibrosis and Autoimmunity in Scleroderma. *Front Immunol*. 2018 Aug 16;9:1896.
- 41-Desallais L, Avouac J, Fréchet M, Elhai M, Ratsimandresy R, Montes M, Mouhsine H, Do H, Zagury JF, Allanore Y. Targeting IL-6 by both passive or active immunization strategies prevents bleomycin-induced skin fibrosis. *Arthritis Res Ther*. 2014 Jul 24;16(4):R157.
- 42-Crescioli C, Corinaldesi C, Riccieri V, Raparelli V, Vasile M, Del Galdo F, Valesini G, Lenzi A, Basili S, Antinozzi C. Association of circulating CXCL10 and CXCL11 with systemic sclerosis. *Ann Rheum Dis*. 2018 Dec;77(12):1845-1846.
- 43-Volkman ER, Tashkin DP, Kuwana M, Li N, Roth MD, Charles J, Hant FN, Bogatkevich GS, Akter T, Kim G, Goldin J, Khanna D, Clements PJ, Furst DE, Elashoff RM, Silver RM, Assassi S. Progression of Interstitial Lung Disease in Systemic Sclerosis: The Importance of Pneumoproteins Krebs von den Lungen 6 and CCL18. *Arthritis Rheumatol*. 2019 Dec;71(12):2059-2067.
- 44-van der Kroef M, Carvalheiro T, Rossato M, de Wit F, Cossu M, Chouri E, Wichers CGK, Bekker CPJ, Beretta L, Vazirpanah N, Trombetta E, Radstake TRDJ, Angiolilli C. CXCL4 triggers monocytes and macrophages to produce PDGF-BB, culminating in fibroblast activation: Implications for systemic sclerosis. *J Autoimmun*. 2020 Jul;111:102444.
- 45-Perelas A, Silver RM, Arrossi AV, Highland KB. Systemic sclerosis-associated interstitial lung disease. *Lancet Respir Med*. 2020 Mar;8(3):304-320.
- 46-Shilling AD, Nedza FM, Emm T, Diamond S, McKeever E, Punwani N, Williams W, Arvanitis A, Galya LG, Li M, Shepard S, Rodgers J, Yue TY, Yeleswaram S. Metabolism, excretion, and pharmacokinetics of [14C]INCB018424, a selective Janus tyrosine kinase 1/2 inhibitor, in humans. *Drug Metab Dispos*. 2010 Nov;38(11):2023-31.
- 47-Dowty ME, Lin J, Ryder TF, Wang W, Walker GS, Vaz A, Chan GL, Krishnaswami S, and Prakash C (2014) The pharmacokinetics, metabolism, and clearance mechanisms of tofacitinib, a janus kinase inhibitor, in humans. *Drug Metab Dispos* 42:759–773.
- 48-Gong X, Darpo B, Xue H, Punwani N, He K, Barbour AM, Epstein N, Landman R, Chen X, Yeleswaram S. Evaluation of Clinical Cardiac Safety of Itacitinib, a JAK1 Inhibitor, in Healthy Participants. *Clin Pharmacol Drug Dev*. 2019 Dec 10 [Epub ahead of print].

- 49-Krishnaswami S, Boy M, Chow V, and Chan G (2015) Safety, tolerability, and pharmacokinetics of single oral doses of tofacitinib, a Janus kinase inhibitor, in healthy volunteers. *Clin Pharmacol Drug Dev* 4:83–88.
- 50-Kawaguchi Y, Waguri-Nagaya Y, Tatematsu N, Oguri Y, Kobayashi M, Nozaki M, Asai K, Aoyama M, Otsuka T. The Janus kinase inhibitor tofacitinib inhibits TNF- α -induced gliostatin expression in rheumatoid fibroblast-like synoviocytes. *Clin Exp Rheumatol*. 2018 Jul-Aug;36(4):559-567.
- 51-Stubbs MC, Burn TC, Sparks R, Maduskuie T, Diamond S, Rupar M, Wen X, Volgina A, Zolotarjova N, Waeltz P, Favata M, Jalluri R, Liu H, Liu XM, Li J, Collins R, Falahatpisheh N, Polam P, DiMatteo D, Feldman P, Dostalík V, Thekkat P, Gardiner C, He X, Li Y, Covington M, Wynn R, Ruggeri B, Yeleswaram S, Xue CB, Yao W, Combs AP, Huber R, Hollis G, Scherle P, Liu PCC. The Novel Bromodomain and Extraterminal Domain Inhibitor INCB054329 Induces Vulnerabilities in Myeloma Cells That Inform Rational Combination Strategies. *Clin Cancer Res*. 2019 Jan 1;25(1):300-311.
- 52-Khanna D, Bush E, Nagaraja V, Koenig A, Khanna P, Young A, Moore J, Fox D, Lafyatis R. Tofacitinib in Early Diffuse Cutaneous Systemic Sclerosis— Results of Phase I/II Investigator-Initiated, Double-Blind Randomized Placebo-Controlled Trial [abstract]. *Arthritis Rheumatol*. 2019; 71 (suppl 10).
- 53-Kitanaga Y, Imamura E, Nakahara Y, Fukahori H, Fujii Y, Kubo S, Nakayamada S, Tanaka Y. In vitro pharmacological effects of peficitinib on lymphocyte activation: a potential treatment for systemic sclerosis with JAK inhibitors. *Rheumatology (Oxford)*. 2019 Nov 25.
- 54-Baker KF, Isaacs JD. Novel therapies for immune-mediated inflammatory diseases: What can we learn from their use in rheumatoid arthritis, spondyloarthritis, systemic lupus erythematosus, psoriasis, Crohn's disease and ulcerative colitis? *Ann Rheum Dis*. 2018 Feb;77(2):175-187.
- 55- Pei H, He L, Shao M, Yang Z, Ran Y, Li D, Zhou Y, Tang M, Wang T, Gong Y, Chen X, Yang S, Xiang M, Chen L. Discovery of a highly selective JAK3 inhibitor for the treatment of rheumatoid arthritis. *Sci Rep*. 2018 Mar 27;8(1):5273.
- 56-Wang Y, Kuai Q, Gao F, Wang Y, He M, Zhou H, Han G, Jiang X, Ren S, Yu Q. Overexpression of TIM-3 in Macrophages Aggravates Pathogenesis of Pulmonary Fibrosis in Mice. *Am J Respir Cell Mol Biol*. 2019 Dec;61(6):727-736.
- 57-Xiong Y, Liu Y, Cao L, Wang D, Guo M, Jiang A, Guo D, Hu W, Yang J, Tang Z, Wu H, Lin Y, Zhang M, Zhang Q, Shi M, Liu Y, Zhou Y, Lan K, Chen Y. Transcriptomic characteristics of bronchoalveolar lavage fluid and peripheral blood mononuclear cells in COVID-19 patients. *Emerg Microbes Infect*. 2020 Dec;9(1):761-770.

- 58-Morin F, Kavian N, Nicco C, Cerles O, Chéreau C, Batteux F. Niclosamide Prevents Systemic Sclerosis in a Reactive Oxygen Species-Induced Mouse Model. *J Immunol*. 2016 Oct 15;197(8):3018-3028.
- 59-Morin F, Kavian N, Chouzenoux S, Cerles O, Nicco C, Chéreau C, Batteux F. Leflunomide prevents ROS-induced systemic fibrosis in mice. *Free Radic Biol Med*. 2017 Jul;108:192-203.
- 60-van der Kroef M, Castellucci M, Mokry M, Cossu M, Garonzi M, Bossini-Castillo LM, Chouri E, Wichers CGK, Beretta L, Trombetta E, Silva-Cardoso S, Vazirpanah N, Carvalheiro T, Angiolilli C, Bekker CPJ, Affandi AJ, Reedquist KA, Bonte-Mineur F, Zirkzee EJM, Bazzoni F, Radstake TRDJ, Rossato M. Histone modifications underlie monocyte dysregulation in patients with systemic sclerosis, underlining the treatment potential of epigenetic targeting. *Ann Rheum Dis*. 2019 Apr;78(4):529-538.
- 61-Bei Y, Hua-Huy T, Nicco C, Duong-Quy S, Le-Dong NN, Tiev KP, Chéreau C, Batteux F, Dinh-Xuan AT. RhoA/Rho-kinase activation promotes lung fibrosis in an animal model of systemic sclerosis. *Exp Lung Res*. 2016;42(1):44-55
- 62-Mowat AM, Scott CL, Bain CC. Barrier-tissue macrophages: functional adaptation to environmental challenges. *Nat Med*. 2017 Nov 7;23(11):1258-1270.
- 63-Jablonski KA, Amici SA, Webb LM, Ruiz-Rosado Jde D, Popovich PG, Partida-Sanchez S, Guerau-de-Arellano M. Novel Markers to Delineate Murine M1 and M2 Macrophages. *PLoS One*. 2015 Dec 23;10(12):e0145342.
- 64-Misharin AV, Morales-Nebreda L, Reyfman PA, Cuda CM, Walter JM, McQuattie-Pimentel AC, et al. Monocyte-derived alveolar macrophages drive lung fibrosis and persist in the lung over the life span. *J Exp Med*. 2017 Aug 7;214(8):2387-2404.
- 65-Lescoat A, Ballerie A, Belhomme N, Cazalets C, de Carlan M, Droitcourt C, Perdriger A, Jégo P, Coiffier G. Synovial involvement assessed by power Doppler ultra-sonography in systemic sclerosis: results of a cross-sectional study. *Rheumatology (Oxford)*. 2018 Nov 1;57(11):2012-2021.
- 66-Stifano G, Christmann RB. Macrophage Involvement in Systemic Sclerosis: Do We Need More Evidence? *Curr Rheumatol Rep*. 2016 Jan;18(1):2
- 67-Bhandari R, Ball MS, Martyanov V, Popovich D, Schaafsma E, Han S, Eltanbouly M, Orzechowski NM, Carns M, Arroyo E, Aren K, Hinchcliff M, Whitfield ML, Pioli PA. Pro-fibrotic Activation of Human Macrophages in Systemic Sclerosis. *Arthritis Rheumatol*. 2020 Mar 5 [Epub ahead of print].
- 68-Lescoat A, Ballerie A, Lelong M, Augagneur Y, Morzadec C, Jouneau S, Jégo P, Fardel O, Vernhet L, Lecureur V. Crystalline Silica Impairs Efferocytosis Abilities of Human and

Mouse Macrophages: Implication for Silica-Associated Systemic Sclerosis. Front Immunol. 2020 Feb 18;11:219.

Legends of Figures

Fig.1. Validation of key polarizations markers of 5 activation states of human MDM:

(A) Evaluation of mRNA expression in M1i (MDM activated by IFN γ) and M1Li (MDM activated by IFN γ and LPS) relative to control M0 (MDM without *in vitro* activation), arbitrarily set to 1 unit (Dashed line). All experiments are the results of triplicate experiments conducted in MDM from n=4 to 6 independent healthy donors and data are expressed as means +/- SEM. \$, P<0.05 in comparison with M0; \$\$, P<0.01 in comparison with M0. (B) Evaluation of cytokine and chemokine secretion levels (pg/ml) in the culture medium of M0, M1i and M1Li MDM by ELISA. All experiments are the results of duplicates experiments conducted in MDM from n=4 to 6 independent healthy donors and are expressed as means +/- SEM. *, P<0.05; **, P<0.01. (C) Evaluation of mRNA expression in M2a (MDM activated by IL-4 and IL-13) relative to control M0 arbitrarily set to 1 (Dashed line). All experiments are the results of triplicate experiments conducted in MDM from n=4 to 6 independent healthy donors and are expressed as means +/- SEM. \$, P<0.05; \$\$, P<0.05 in comparison with M0. (D) Evaluation of cytokine and chemokine secretion levels (pg/ml) in the culture medium of M0 and M2a MDM by ELISA. All experiments are the results of duplicates experiments conducted in MDM from n=4 to 6 independent healthy donors and are expressed as means +/- SEM. *, P<0.05; **, P<0.01 (E) Evaluation of mRNA expression in M2c (MDM activated by IL-10) and M2c+dex (MDM activated by IL-10 and dexamethasone) relative to control M0 arbitrarily set to 1 (Dashed line). All experiments are the results of triplicate experiments conducted in MDM from n=4 to 6 independent healthy donors and are expressed as means +/- SEM. \$, P<0.05; \$\$, P<0.01 in comparison with M0. (F) Comparison of membrane expression of key polarization markers in all considered activation states by flow cytometry. Experiments were conducted in

MDM from n=4 to 6 independent healthy donors and data are expressed as means +/- SEM of ratio of MFI. *, P<0.05; **, P<0.01; ***, P<0.001.

Fig.2. Impact of ruxolitinib (Ruxo), tofacitinib (Tofa) and itacitinib (Ita) on cell viability of unpolarized and polarized human MDM: MDM were pre-treated for 1 h with 1 or 0.1 μ M of ruxolitinib (A), tofacitinib (B) or itacitinib (C) and then unpolarized (M0) or polarized into M1i, M1Li, M2a, M2c or M2c+dex MDM for additional 20 h. Cell viability was then assessed through WST1 assay. All experiments are the results of duplicate experiments conducted in MDM from n=4 independent healthy donors and are expressed as means +/- SEM. *, P<0.01, in comparison with unpolarized M0 MDM exposed to DMSO, arbitrarily set to 100% (Dashed line).

Fig.3. Impact of ruxolitinib (Ruxo), tofacitinib (Tofa) and itacitinib (Ita) on the polarization state of M1i and M1Li human MDM: (A and B) Evaluation of mRNA expression in M1i and M1Li after treatment by the three considered JAK inhibitors (1 μ M). All experiments are the results of triplicate experiments conducted in MDM from n=4 to 6 independent healthy donors and are expressed as means +/- SEM. \$, P<0.05; \$\$, P<0.01; \$\$\$, P<0.001 in comparison with M1i or M1Li arbitrarily set to 1 (Dashed line); *, P<0.05; ** P<0.01; ***, P<0.001 expressing differences among the different JAK inhibitors. (C and D) Evaluation of cytokine and chemokine secretion levels (pg/ml) in the culture medium of M1i and M1Li MDM or the three considered JAK inhibitors (1 μ M) by ELISA. All experiments are the results of duplicates experiments conducted in MDM from n=4 to 6 independent healthy donors and are expressed as means +/- SEM. *P<0.05. (E and F) Comparison of membrane expression of key polarization markers in M1i or M1Li, treated with DMSO or the three considered JAK inhibitors (1 μ M) by flow cytometry. Experiments were conducted in MDM

from n=3 to 5 independent healthy donors and data are expressed as means +/- SEM of ratio of MFI. *, P<0.05; **, P<0.01; ***, P<0.001.

Fig.4. Impact of two concentrations of ruxolitinib (Ruxo), tofacitinib (Tofa) and itacitinib (Ita) on five activations states of human MDM: (A) Evaluation of mRNA expression in M2a after treatment by the three considered JAK inhibitors (1 μ M). All experiments are the results of triplicate experiments conducted in MDM from n=4 to 6 independent healthy donors and are expressed as means +/- SEM. \$, P<0.05; \$\$, P<0.01; \$\$\$, P<0.01 in comparison with control M2a treated with DMSO, arbitrarily set to 1 unit (Dashed line). *, P<0.05; **, P<0.01; ***, P<0.001 expressing differences among the independent JAK inhibitors (1 μ M). (B) Evaluation of cytokine and chemokine secretion levels (pg/ml) in the culture medium of M2a MDM treated with DMSO or the three considered JAK inhibitors (1 μ M) by ELISA. All experiments are the results of duplicates experiments conducted in MDM from n=4 to 6 independent healthy donors and are expressed as means +/- SEM. ***, P<0.001 (C) Comparison of membrane expression of CD206, a key polarization marker of M2a activation, after treatment with DMSO or the three considered JAK inhibitors (1 μ M) by flow cytometry. Experiments conducted in MDM from n=5 independent healthy donors and data are expressed as means +/- SEM of ratio of MFI. *, P<0.05; **, P<0.01; ***, P<0.001.

Fig.5. Impact of ruxolitinib (Ruxo), tofacitinib (Tofa) and itacitinib (Ita) on the polarization state of M2c and M2c+dex human MDM: (A and C) Evaluation of relative transcript expression in M2c after treatment by the three considered JAK inhibitors (1 μ M and 0.1 μ M). All experiments are the results of triplicate experiments conducted in MDM from n=4 to 6 independent healthy donors and data are expressed as means +/- SEM. \$, P<0.05; \$\$, P<0.01; \$\$\$, P<0.01 in comparison with M2c treated with solvent (DMSO) arbitrarily set to 1

(Dashed line); *, $P < 0.05$; **, $P < 0.01$; ***, $P < 0.001$ expressing differences among the different JAK inhibitors. **(B and D)** Comparison of membrane expression of CD163, a key polarization marker of M2c activation, after treatment with DMSO or the three considered JAK inhibitors (1 μM and 0.1 μM) by flow cytometry. Experiments conducted in MDM from $n=3$ to 5 independent healthy donors and data are expressed as means \pm SEM of ratio of MFI. *, $P < 0.05$. **(E and F)** Evaluation of relative transcripts expression in M2c+dex after treatment by the three considered JAK inhibitors (1 μM and 0.1 μM). All experiments are the results of triplicate experiments conducted in MDM from $n=4$ to 6 independent healthy donors and data are expressed as means \pm SEM. \$\$, $P < 0.01$; \$\$\$, $P < 0.001$ in comparison with M2c+dex treated with DMSO arbitrarily set to 1 (Dashed line); *, $P < 0.05$; **, $P < 0.01$; ***, $P < 0.001$ expressing differences among the different JAK inhibitors. **(G and H)** Flow cytometry-based comparison of membrane expression of CD204, a key polarization marker of M2c+dex activation, after treatment with DMSO or the three considered JAK inhibitors (1 μM and 0.1 μM). Experiments were conducted in MDM from $n=3$ to 5 independent healthy donors and data are expressed as means \pm SEM of ratio of MFI.

Fig.6. Heatmap summarizing the impact of two concentrations of ruxolitinib (Ruxo), tofacitinib (Tofa) and itacitinib (Ita) on five activation states of human MDM: Heatmap represents data expressed as the mean-fold of qPCR experiments (from $n=4$ to 6 independent healthy donors) and flow cytometry experiments (from $n=3$ to 5 independent healthy donors) conducted in MDM exposed to 0.1 or 1 μM of ruxolitinib, tofacitinib or itacitinib, and then polarized into M1i, M1Li, M2a, M2c or M2c+dex MDM for additional 20 h.

Fig.7. Impact of ruxolitinib (Ruxo) on the phosphorylation state of key STAT involved in each polarization state of human MDM: MDM were exposed to 1 μM of ruxolitinib or to

DMSO for 1 h and then unpolarized (M0) or polarized into M1i or MILi (A), M2a (B), M2c or M2c+dex (C) for additional 2 h. Cells were lysed and expressions of phospho-STAT1 (A), phospho-STAT6 (B) or phospho-STAT3 (C) were analyzed by Western blotting. Images presented are representative of at least four independent experiments on independent health donors. Phospho-STAT-related stained bands were quantified by densitometric analysis and expressed relatively to expression level found in untreated M0 MDM, arbitrarily set to the value of 100%, after normalization to GAPDH content. Experiments were conducted in MDM from n=4 to 5 independent healthy donors and data are expressed as means +/- SEM. \$, P<0.05; \$\$, P<0.01; \$\$\$, P<0.01 in comparison with M0 treated with DMSO arbitrarily set to 1. *, P<0.05, **, P<0.01, ***, P<0.001 in comparison to their respective untreated polarization state.

Fig.8. Impact of ruxolitinib (Ruxo) on skin lesions in a mouse model of HOCl-induced Systemic Sclerosis (SSc). (A&B) Transcript relative expressions of key M1 and M2 polarization markers of mouse macrophages in the skin after 3 and 6 weeks of intradermal injection. \$, P<0.05; \$\$, P<0.01; \$\$\$, P<0.01 in comparison with the PBS control group arbitrarily set to 1 (Dashed line); * P<0.05; **, P<0.01; ***, P<0.01 expressing differences between the group HOCl treated with solvent and group HOCl treated with ruxolitinib (n=8-9 mice per group). Results are expressed as means +/- SEM. (C&D) Impact of ruxolitinib on skin thickness after Masson's trichrome and Sirius red stainings respectively. (E) Data of biopsy weight (mg) are expressed by the means +/- SEM (n=8-9 mice per group). (F) Data of skin thickness (μm , 6 measures per mice) are expressed by the means +/- SEM (n=8-9 mice per group).

Fig.9. Impact of ruxolitinib (Ruxo) on SSc-associated interstitial lung disease in a mouse model of HOCl-induced Systemic Sclerosis (SSc), after 6 weeks of intradermal injection.

Staining of lung (left upper lobe) showing total section (x1,25) and details of the sub-pleural, parenchymal and peri-bronchial regions (x20) by Masson's Trichrome (A) or by Sirius red (B). Sections of mouse lung are representative of each group (n=8-9 mice per group). (C) Hydroxyproline content per lung lobe is expressed as means +/- SEM. *P<0.05, (n=8-9 mice per group). (D) The mRNA relative expressions of key pro-fibrotic markers in the lungs after 6 weeks of intradermal injections are expressed as means +/- SEM. \$, P<0.05; \$\$, P<0.01; \$\$\$, P<0.01 in comparison with the PBS control group arbitrarily set to 1 (Dashed line); *, P<0.05; **, P<0.01; ***, P<0.01 expressing differences between the group HOCl treated with solvent and group HOCl treated with ruxolitinib (n=8-9 mice per group). (E) Section of sub-pleural infiltrate, Masson's Trichrome stained sections (x40). Sections of mouse lung representative of each group (n=8-9 mice per group). (F) The mRNA relative expressions of key M1 and M2 polarization markers of mouse macrophages in the lungs after 6 weeks of intradermal injections are expressed as means +/- SEM. \$, P<0.05; \$\$, P<0.01; \$\$\$, P<0.01 in comparison with the PBS control group arbitrarily set to 1 (Dashed line); *, P<0.05; **, P<0.01; ***, P<0.01 expressing differences between the groups HOCl treated with solvent and HOCl treated with ruxolitinib (n=8-9 mice per group).

BIOCHEMICAL PHARMACOLOGY

Category: Inflammation and Immunopharmacology

Full-length Research Article

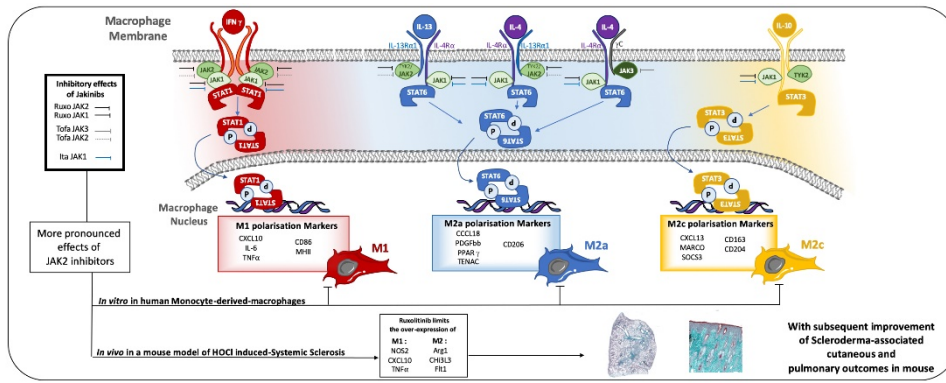
Combined anti-fibrotic and anti-inflammatory properties of JAK-inhibitors on macrophages in vitro and in vivo: perspectives for scleroderma-associated interstitial lung disease.

Alain LESCOAT^{1,2}, Marie LELONG¹, Mohamed JELJELI^{3,4}, Claire PIQUET-PELLORCE¹, Claudie MORZADEC¹, Alice BALLERIE^{1,2}, Stéphane JOUNEAU^{1,5}, Patrick JEGO^{1,2}, Laurent VERNHET¹, Frédéric BATTEUX^{3,4}, Olivier FARDEL^{1,6} and Valérie LECUREUR^{1*}

Credit authorship contribution statement

Alain Lescoat: Conceptualization, Validation, Formal analysis, Investigation, Writing, Visualization, Funding acquisition. **Marie Lelong:** Validation, Investigation. **Mohamed Jeljeli:** Methodology, Resources. **Claire Piquet-Pellorce:** Investigation, Methodology. **Claudie Morzadec:** Investigation, Resources. **Alice Ballerie:** Writing, Visualization, Funding acquisition. **Stéphane Jouneau:** Writing, Visualization, Funding acquisition. **Patrick Jégo:** Resources, Funding acquisition. **Laurent Vernhet:** Resources, Conceptualization, Writing. **Frédéric Batteux:** Methodology, Resources. **Olivier Fardel:** Conceptualization, Writing, Funding acquisition. **Valérie Lecureur:** Conceptualization, Validation, Formal analysis, Investigation, Writing, Supervision, Funding acquisition.





Journal Pre-proofs